Laser and Particle Beams (2008), *26*, 591–596. Printed in the USA.

doi:10.1017/S0263034608000657

Effects of front surface plasma expansion on proton acceleration in ultraintense laser irradiation of foil targets

P. MCKENNA,[1] D.C. CARROLL,[1] O. LUNDH,[2] F. NÜRNBERG,[3] K. MARKEY,[4]
S. BANDYOPADHYAY,[5] D. BATANI,[6] R.G. EVANS,[7] R. JAFER,[6] S. KAR,[4] D. NEELY,[5] D. PEPLER,[5]
M.N. QUINN,[1] R. REDAELLI,[6] M. ROTH,[3] C.-G. WAHLSTRÖM,[2] X.H. YUAN,[1] AND M. ZEPF[4]

[1]SUPA, Department of Physics, University of Strathclyde, Glasgow, United Kingdom
[2]Department of Physics, Lund University, Lund, Sweden
[3]Technische Universität Darmstadt, Institut für Kernphysik, Darmstadt, Germany
[4]School of Mathematics and Physics, Queen's University Belfast, Belfast, United Kingdom
[5]STFC, Rutherford Appleton Laboratory, Didcot, United Kingdom
[6]Dipartimento di Fisica, Università di Milano Bicocca, Milano, Italy
[7]The Blackett Laboratory, Imperial College London, London, United Kingdom

(RECEIVED 14 July 2008; ACCEPTED 1 October 2008)

Abstract

The properties of beams of high energy protons accelerated during ultraintense, picosecond laser-irradiation of thin foil targets are investigated as a function of preplasma expansion at the target front surface. Significant enhancement in the maximum proton energy and laser-to-proton energy conversion efficiency is observed at optimum preplasma density gradients, due to self-focusing of the incident laser pulse. For very long preplasma expansion, the propagating laser pulse is observed to filament, resulting in highly uniform proton beams, but with reduced flux and maximum energy.

Keywords: Laser-plasma interaction; Laser-proton acceleration; Plasma expansion

INTRODUCTION

The generation of beams of multi-MeV ions in the interaction of high power laser pulses with thin foil targets continues to attract considerable international interest, due to the uniquely short pulse and low emittance properties of the beam, and the potentially compact nature of the source (Borghesi *et al.*, 2006; Badziak, 2007; Flippo *et al.*, 2007; Schollmeier *et al.*, 2007; Nickles *et al.*, 2007; Faenov *et al.*, 2007; Strangio *et al.*, 2007; McKenna *et al.*, 2007). At the laser intensities available at present, the main ion acceleration occurs at the rear of the target and is driven by relativistic electrons accelerated at the front, irradiated surface, that propagate through the target and produce an electrostatic sheath at the rear surface (Wilks *et al.*, 2001). The main ion species accelerated is the proton, due to its high charge-to-mass ratio and the presence of hydrogenated contamination layers on the target surfaces (Hegelich *et al.*, 2002; McKenna *et al.*, 2004). The challenge, for potential applications of this unique source, is to enhance and control the source and beam properties.

Preplasma, which is typically produced by prepulses and amplified spontaneous emission (ASE) at the leading edge of a high power laser pulse, can play a significant role in defining the properties of the ion beam. It has been shown that prepulse induced heating and expansion of the target rear surface reduces the maximum proton energy (Roth *et al.*, 2002; Fuchs *et al.*, 2007). Furthermore, Kaluza *et al.* (2004) report that the optimum target thickness for proton acceleration strongly depends on prepulse duration and Lindau *et al.* (2005) report proton beam steering due to ASE-driven target rear surface deformation. However, even for conditions for which the target rear surface is unperturbed, plasma expansion at the front surface can significantly affect rear surface ion acceleration. Recent, theoretical studies have shown that by controlling the scale length of the front surface preplasma, laser absorption efficiency, and therefore proton acceleration, can be enhanced (Sentoku *et al.*, 2002; Seo *et al.*, 2007; Lee *et al.*, 2004; Andreev *et al.*, 2006). Proton energy enhancement at laser intensities between 10^{18} and 10^{19} W/cm^2, where the effect is predicted to be most pronounced (Sentoku *et al.*, 2002),

Address correspondence and reprint requests to: Paul McKenna, SUPA, Department of Physics, University of Strathclyde, Glasgow G4 0NG, United Kingdom. E-mail: p.mckenna@phys.strath.ac.uk

has been observed using ultrashort (tens of femtosecond) laser pulses (Maksimchuk *et al.*, 2000; Yogo *et al.*, 2007; Glinec *et al.*, 2008).

In this paper, we report on the effects of controlled front surface plasma expansion on proton acceleration at the rear of thin metallic foils in the ultraintense picosecond laser pulse regime. It is in this regime of intensity and pulse duration that the highest energy protons are presently produced (Snavely *et al.*, 2000; Robson *et al.*, 2007). This regime is also directly relevant to the fast ignition approach to fusion energy (Tabak *et al.*, 1994; Sakagami *et al.*, 2006). That scheme involves a laser pulse, with similar parameters, that propagates through coronal plasma and delivers energy, usually in the form of fast electrons, inside a precompressed deuterium-tritium pellet.

EXPERIMENTAL

The experiment is performed using the Vulcan petawatt laser at the Rutherford Appleton Laboratory (Danson *et al.*, 2005). Chirped pulse amplified (CPA) 1054 nm wavelength (λ) light, in pulses with duration equal to 1 ps (full width at half maximum (FWHM)) is used to accelerate protons. A plasma mirror (Dromey *et al.*, 2004), positioned in the focusing beam, suppresses the intensity of the ASE pedestal to $\sim 10^{11}$ W/cm^2. The mirror is operated at 20° angle of incidence, in a *p*-polarized geometry, with a measured reflectivity of 32%, providing a maximum energy on target of 115 J. The CPA pulses are incident on target at 10° and focused to a spot size of 5 μm (FWHM), to achieve a calculated peak intensity, I_{CPA}, equal to 3×10^{20} W/cm^2.

The expanding preplasma is produced using low energy "ablation" laser pulses of 6 ns duration (with a fast rise time of 0.2 ns and slow decay to about 50% of the peak intensity at 6 ns) and wavelength equal to 1053 nm. The pulses are focused, using an $f/10$ lens, to an approximately flat-top intensity distribution of 450 μm diameter on the target front surface, centered at the same position as the CPA focus. The pulse energy is controlled to vary the intensity, I_{abl}, in the range 0.5 to 5 TW/cm^2. The ablation pulse arrives on target first, and the time delay of the arrival of the CPA pulse, Δt, is varied in the range 0.5 to 3.6 ns, with 0.2 ns precision.

The targets are 25 μm-thick planar Cu foils or 25 μm-thick Au foils with a periodic groove structure (lines) on the rear surface. The lines have a period of 10 μm and a peak-to-valley depth of 1.1 μm, with a sinusoidal profile.

The spatial and energy distributions of the beam of accelerated protons are measured using a passive stack of dosimetry film (Gafchromic© film, HD-810 and MD-V2-55). The plasma expansion is characterized by application of interferometry (Benattar *et al.*, 1979) on a 527 nm wavelength probe beam directed across the target. Interferograms are recorded with a 16 bit CCD camera, 5 ps after the arrival of the CPA pulse, and with a spatial resolution of 5 μm.

RESULTS

The main findings of our investigation result from changes to the spectral and spatial intensity distributions of the proton beam measured at the rear of the target. The beam parameters are measured as a function of (1) I_{abl} for fixed $\Delta t = 0.5$ ns, and (2) Δt for fixed $I_{abl} = 1$ TW/cm^2, for otherwise identical CPA pulse and target parameters. Figure 1a shows example proton energy spectra from a scan of I_{abl}. The measured scale length of the electron density, along the target normal, in the *underdense* region of the expanding plasma at the target front surface is marked for each plot. Hereafter, we refer to this, the scale length of the *outer* part of the preplasma, as L_O, and we refer to the density scale length in the *inner* region, near the critical density, as L_I. L_O is determined by fitting the relation $n_e(x) \propto \exp(-x/L_O)$ (where n_e is the electron density and x is the distance from the target surface) to the electron density profile extracted from the interferometric probe measurements. As shown in Figures 1b and 1c, as L_O is increased from ~0 (no ablation pulse) to ~60 μm, the maximum proton energy, E_{max}, increases by about 25% and the efficiency of conversion, η, of laser energy to protons (above a lower detection threshold of 2.4 MeV) increases by about 50%. The proton "temperature," T, is also observed to increase, by about 40%, from 3.5 to 4.8 MeV over this range. As L_O is increased beyond 100 μm, E_{max}, T, and η all decrease below their respective values for the case of a sharp density gradient. The same dependency on L_O is measured whether the preplasma scale length is varied by changing I_{abl} or Δt, as clearly observed in Figures 1b and 1c.

Whereas there is an optimum preplasma expansion to enhance E_{max}, T, and η, improvements in the spatial-intensity profile of the proton beam are observed for all cases in which a preplasma expansion is produced by the ablation pulse, with the most uniform proton beams measured for the longest preplasma scale lengths. In agreement with previous observations reported in Carroll *et al.* (2007), we measure significant improvements in the uniformity and circularity of the beam over the full proton energy range. For example, in a sample region corresponding to 50% of the beam area, in the center of the beam, the standard deviation of the proton dose at 10 MeV decreases from 36% of the mean value, in the absence of the ablation pulse, to 19% for $L_O = 145$ μm. The deviation of the spatial profile of the proton beam from a perfect circle (circularity measured as $4\pi \cdot Area/(Circumference)^2$) decreases from 4% to 1% for the same sample proton dose distributions. Using targets with a periodic groove structure on the rear surface, we determine, from the number of lines reproduced in the proton spatial intensity profiles, the proton source size decreases with increasing proton energy, from ~600 μm at 4 MeV to ~50 μm at 30 MeV in the absence of an ablation pulse. An increase of between 20% and 50% is measured, at all energies, for $I_{abl} = 0.5$ TW/cm^2 ($L_O = 38$ μm), and as I_{abl} is increased to 5.0 TW/cm^2 ($L_O = 145$ μm), the

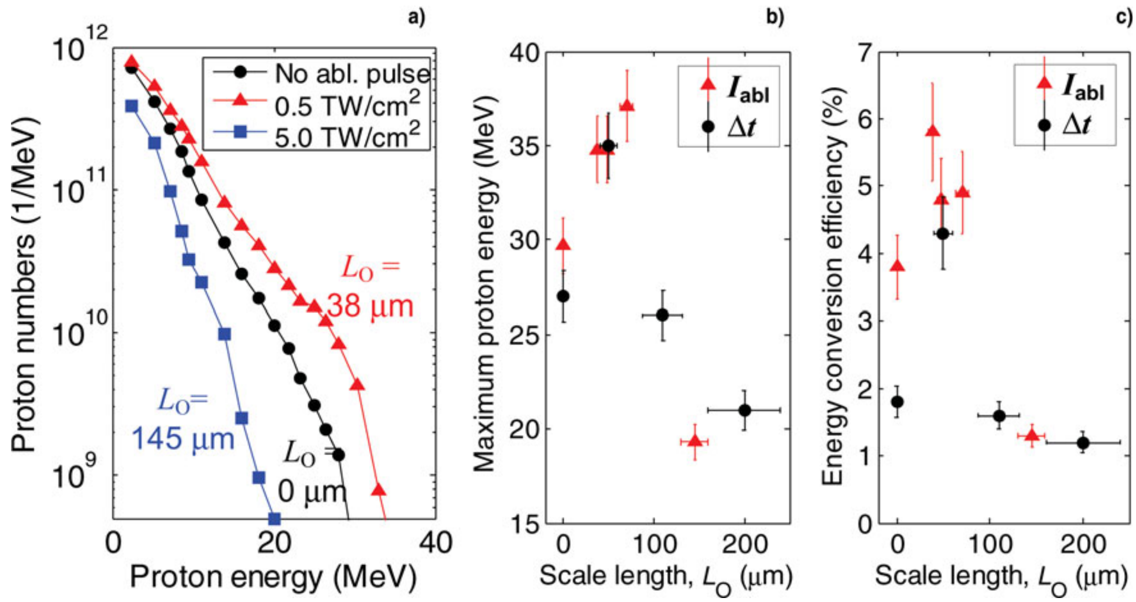

Fig. 1. (**a**) Example proton energy spectra, measured using stacked dosimetry films, for different I_{abl} and fixed $\Delta t = 0.5$ ns; (**b**) Maximum proton energy, and (**c**) Laser-to-proton energy conversion efficiency as a function of L_O, obtained for different I_{abl} up to 5.0 TW/cm^2 for fixed $\Delta t = 0.5$ ns (triangles), and for different Δt up to 3.6 ns for fixed $I_{abl} = 1.0$ TW/cm^2 (circles).

source size is reduced by a factor of two. We do not observe a significant change to the proton beam normalized transverse emittance, measured using the technique described by Cowan *et al.* (2004). Typically, we obtain values of the order of 0.011 π mm mrad at example proton energy of 6 MeV.

We measure the density profile in the preformed plasma at the target front surface up to an electron density limit of $\sim 4 \times 10^{19}$ cm^{-3} due to refraction at the steep density gradients. In order to determine the full initial density profile, two-dimensional hydrodynamic simulations are performed using the Pollux code (Pert, 1981). Cylindrical symmetry is used with a 300 µm by 300 µm grid with cell size equal to 1.5 µm. The target material is Cu. The laser wavelength and spot radius are set at 1.06 µm and 220 µm, respectively, and the pulse has a rise time of 0.2 ns and thereafter remains at a chosen intensity. Two distinct regions of preplasma expansion, with scale lengths L_I and L_O, are clearly observed in the example results in Figure 2a. These calculated density profiles are in good agreement with the corresponding measured profiles (also shown). The simulation results predict an increase in L_O from 31 µm to 182 µm for an increase in Δt from 0.5 ns to 3.5 ns, for fixed $I_{abl} = 1$ TW/cm^2, and the corresponding measured values are 50 ± 10 µm and 200 ± 40 µm, respectively. From the simulation results we infer that L_I, in the region of the relativistically corrected critical density ($\sim 11 n_c$), increases from ~ 0.6 µm to ~ 0.9 µm for an increase in Δt from 0.5 to 3.5 ns. The small increase (4%) in the thickness of the overdense region of the target is expected to have negligible effect on the proton acceleration.

Importantly, there is evidence from four independent sources that expansion of the target rear surface does not occur prior to the arrival of the CPA pulse on target. Calculation of the position of the shock front, launched by the ablation pulse, using the approach and parameters given in Lundh *et al.* (2007), indicates that it does not reach the target rear surface for the parameter range experimentally investigated. This is confirmed by the hydrodynamic simulation results, as shown in the inset of Figure 2a. The absence of target rear surface expansion is confirmed experimentally in the interferograms, within the limit of the spatial resolution. Finally, the periodic structure on the rear surface of the Au targets is clearly observed in the proton beam spatial intensity profile, indicating that the structure is unperturbed prior to the arrival of the CPA pulse.

From the transverse optical probe measurements we conclude that the observed changes to the proton beam result from changes to the CPA laser pulse propagation in the expanding plasma. For some laser shots, for the conditions of optimum E_{max}, T, and η, a single channel, with width smaller than the nominal focusing cone of the CPA beam, is observed, Figure 2b, and is evidence of self focusing of the beam. This results in a smaller focal spot, and hence a higher I_{CPA}, compared to the case of a steep density gradient. By contrast, for very long scale length expansion ($L_O >$ 100 µm), typically the CPA beam is observed to filament, Figure 2c, reducing I_{CPA}. The measured changes in E_{max} and T are consistent with the inferred qualitative changes in I_{CPA}. The measured changes in η suggest enhanced laser energy absorption for optimum plasma expansion conditions, at which channeling of the CPA laser pulse is observed.

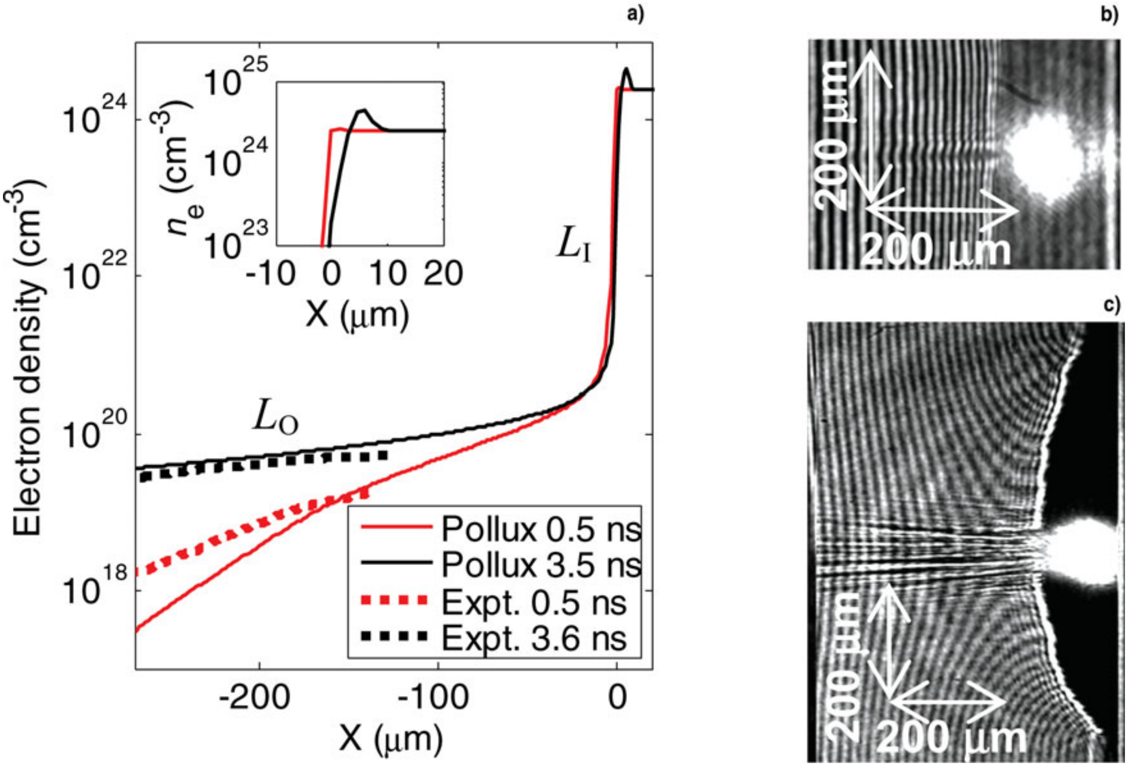

Fig. 2. (**a**) Electron density profiles at the front surface of a Cu target for different expansion times (0.5 ns and ~3.5 ns) at fixed I_{abl} = 1 TW/cm^2: solid lines are calculated using the Pollux hydrodynamic code; dashed lines are experimental measurements obtained from the interferograms. X = 0 corresponds to the initial target front surface. The inset is an enlarged region to show the extent of shock propagation in the target; (**b**) Example interferometric probe image showing channelling of the CPA laser beam in relatively short scale length preplasma; (**c**) Example interferometric probe image showing filamentation of the CPA laser beam in long scale length preplasma. The laser pulses are incident from the left in (b) and (c), and self emission at the critical surface is observed.

The proton beam uniformity is sensitive to a number of parameters, including the profile of the CPA laser focus, the angular distribution of the fast electrons generated, and the extent of small-angle scattering of the fast electrons as they propagate through the target (Fuchs *et al.*, 2003; Schollmeier *et al.*, 2008). The mechanism by which the spatial intensity distribution of the proton beam is influenced by preplasma expansion is a subject for further investigation.

SUMMARY

We have directly measured the effects of front surface plasma expansion on the coupling of laser energy to protons (*via* fast electrons) for laser pulse parameters directly relevant to the fast ignitor scheme. We have demonstrated that, compared to a sharp density gradient, a preplasma with an underdense scale length of ~30 to 60 μm enhances proton acceleration due to self-focusing of the laser beam. The measured ~25% enhancement in the maximum energy, for $I_{CPA} = 3 \times 10^{20}$ W/cm^2, can be compared with the 40% enhancement predicted by Sentoku *et al.* (2002) for a laser intensity of 2.4×10^{20} W/cm^2 (for $\lambda = 1.054$ μm). As the preplasma scale length increases to >100 μm the propagating laser pulse filaments, reducing the laser intensity and giving rise to increased proton beam uniformity, but with reduced energy and flux. The results highlight that properties of the proton beam (and therefore the electron source) can be actively manipulated by optical control of the plasma expansion.

ACKNOWLEDGEMENTS

We acknowledge fruitful discussions with Dr. A.P.L. Robinson and the expert support of the staff at the Central Laser Facility. This work was supported by the UK Engineering and Physical Sciences Research Council (EPSRC Grant number EP/E048668/1), the EU COST P-14 Action and the virtual institute VI-VH-144 (VIPBUL), funded by the Helmholtz Association.

REFERENCES

Andreev, A.A., Sonobel, R., Kawatal, S., Miyazaki, S., Sakai, K., Miyauchi, K., Kikuchi, T., Platonov, K.Y. & Nemoto, K. (2006). Effect of a laser prepulse on fast ion generation in the interaction of ultra-short intense laser pulses with a limited-mass foil target. *Plasma Phys. Contr. Fusion* **48**, 1605–1619.

Badziak, J. (2007). Laser-driven generation of fast particles. *Opto-electr. Rev*. **15**, 1–12.

Benattar, R., Popovics, C. & Sigel, R. (1979). Polarized light interferometer for laser fusion studies. *Rev. Scientif. Instr*. **50**, 1583–1585.

Borghesi, M., Fuchs, J., Bulanov, S.V., Mackinnon, A.J., Patel, P.K. & Roth, M. (2006). Fast ion generation by high-intensity laser irradiation of solid targets and applications. *Fusion Sci. Techn*. **49**, 412–439.

Carroll, D.C., McKenna, P., Lundh, O., Lindau, F., Wahlström, C.-G., Bandyopadhyay, S., Pepler, D.A., Neely, D., Kar, S., Simpson, P., Markey, K., Zepf, M., Bellei, C., Evans, R.G., Redaelli, R. & Batani, D. (2007). Active manipulation of the spatial energy distribution of laser accelerated proton beams. *Phys. Rev. E* **76**, 065401.

Cowan, T., Fuchs, J., Ruhl, H., Kemp, A., Audebert, P., Roth, M., Stephens, R., Barton, I., Blazevic, A., Brambrink, E., Cobble, J., Fernandez, J., Gauthier, J.C., Geissel, M., Hegelich, M., Kaae, J., Karsch, S., Le Sage, G.P., Letzring, S., Manclossi, M., Meyroneinc, S., Newkirk, A., Pepin, H. & Renard-Legalloudec, N. (2004). Ultralow emittance, multi-MeV proton beams from a laser virtual-cathode plasma accelerator. *Phys. Rev. Lett*. **92**, 204801.

Danson, C.N., Brummitt, P.A., Clarke, R.J., Collier, J., Fell, B., Frackiewicz, A.J., Hawkes, S., Hernandez-Gomez, C., Holligan, P., Hutchinson, M.H.R., Kidd, A., Lester, W.J., Musgrave, I.O., Neely, D., Neville, D.R., Norreys, P.A., Pepler, D.A., Reason, C., Shaikh, W., Winstone, T.B., Wyatt, R.W.W. & Wyborn, B.E. (2005). Vulcan petawatt: Design operation and interactions at 5×10^{20} W cm^{-2}. *Laser Part. Beams* **23**, 87–93.

Dromey, B., Kar, S., Zepf, M. & Foster, P.S. (2004). The plasma mirror – A subpicosecond optical switch for ultrahigh power lasers. *Rev. Scientif. Instr*. **75**, 645–649.

Faenov, A.Y., Magunov, A.I., Pikuz, T.A., Skobelev, I.Y., Gasilov, S.V., Stagira, S., Calegari, F., Nisoli, M., De Silvestri, S., Poletto, L., Villoresi, P. & Andreev, A.A. (2007). X-ray spectroscopy observation of fast ions generation in plasma produced by short low-contrast laser pulse irradiation of solid targets. *Laser Part. Beams* **25**, 267–275.

Flippo, K., Hegelich, B.M., Albright, B.J., Yin, L., Gautier, D.C., Letzring, S., Schollmeier, M., Schreiber, J., Schulze, R. & Fernandez, J.C. (2007). Spectral control, monoenergetic ions and new acceleration mechanisms. *Laser Part. Beams* **25**, 3–8.

Fuchs, J., Cecchetti, C.A., Borghesi, M., Grismayer, T., D'humieres, E., Antici, P., Atzeni, S., Mora, P., Pipahl, A., Romagnani, L., Schiavi, A., Sentoku, Y., Toncian, T., Audebert, P. & Willi, O. (2007). Laser-foil acceleration of high-energy protons in small-scale plasma gradients. *Phys. Rev. Lett*. **99**, 015002.

Fuchs, J., Cowan, T., Audebert, P., Ruhl, H., Gremillet, L., Kemp, A., Allen, M., Blazevic, A., Gauthier, J.C., Geissel, M., Hegelich, B.M., Karsch, S., Parks, P., Roth, M., Sentoku, Y., Stephens, R. & Campbell, E.M. (2003). Spatial uniformity of laser-accelerated ultrahigh-current MeV electron propagation in metals and insulators. *Phys. Rev. Lett*. **91**, 255002.

Glinec, Y., Genoud, G., Lundh, O., Persson, A. & Wahlström, C.-G. (2008). Evolution of energy spectrum from laser-accelerated protons with a 100 fs intense prepulse. *Appl. Phys. B* In press.

Hegelich, M., Karsch, S., Pretzler, G., Habs, D., Witte, K.J., Guenther, W., Allen, M., Blazevic, A., Fuchs, J., Gauthier, J.C., Geissel, M., Audebert, P., Cowan, T. & Roth, M. (2002). MeV ion jets from short-pulse-laser interaction with thin foils. *Phys. Rev. Lett*. **89**, 085002.

Kaluza, M., Schreiber, J., Santala, M.I.K., Tsakiris, G.D., Eidmann, K., Meyer-Ter-Vehn, J. & Witte, K.J. (2004). Influence of the laser prepulse on proton acceleration in thin-foil experiments. *Phys. Rev. Lett*. **93**, 045003.

Lee, H.J., Pae, K.H., Suk, H. & Hahn, S.J. (2004). Enhancement of high-energy ion generation by preplasmas in the interaction of an intense laser pulse with overdense plasmas. *Phys. Plasmas* **11**, 1726–1729.

Lindau, F., Lundh, O., Persson, A., McKenna, P., Osvay, K., Batani, D. & Wahlström, C.-G. (2005). Laser-accelerated protons with energy dependent beam direction. *Phys. Rev. Lett*. **95**, 175002.

Lundh, O., Lindau, F., Persson, A., Wahlström, C.-G., McKenna, P. & Batani, D. (2007). Influence of shock waves on laser-driven proton acceleration. *Phys. Rev. E* **76**, 026404.

Maksimchuk, A., Gu, S., Flippo, K. & Umstadter, D. (2000). Forward ion acceleration in thin films driven by a high-intensity laser. *Phys. Rev. Lett*. **84**, 4108–4111.

McKenna, P., Ledingham, K.W.D., Yang, J.M., Robson, L., McCanny, T., Shimizu, S., Clarke, R.J., Neely, D., Spohr, K., Chapman, R., Singhal, R.P., Krushelnick, K., Wei, M.S. & Norreys, P.A. (2004). Characterization of proton and heavier ion acceleration in ultrahigh-intensity laser interactions with heated target foils. *Phys. Rev. E* **70**, 036405.

McKenna, P., Lindau, F., Lundh, O., Carroll, D.C., Clarke, R.J., Ledingham, K.W.D., McCanny, T., Neely, D., Robinson, A.P.L., Robson, L., Simpson, P.T., Wahlström, C.-G. & Zepf, M. (2007). Low- and medium-mass ion acceleration driven by petawatt laser plasma interactions. *Plasma Phys. Contr. Fusion* **49**, B223.

Nickles, P.V., Ter-Avetisyan, S., Schnuerer, M., Sokollik, T., Sandner, W., Schreiber, J., Hilscher, D., Jahnke, U., Andreev, A. & Tikhonchuk, V. (2007). Review of ultrafast ion acceleration experiments in laser plasma at Max Born Institute. *Laser Part. Beams* **25**, 347–363.

Pert, G.J. (1981). Algorithms for the self-consistent generation of magnetic fields in plasmas *J. Computat. Phys*. **43**, 111–163.

Robson, L., Simpson, P.T., Clarke, R.J., Ledingham, K.W.D., Lindau, F., Lundh, O., McCanny, T., Mora, P., Neely, D., Wahlström, C.-G., Zepf, M. & McKenna, P. (2007). Scaling of proton acceleration driven by petawatt-laser-plasma interactions. *Nat. Phys*. **3**, 58–62.

Roth, M., Blazevic, A., Geissel, M., Schlegel, T., Cowan, T.E., Allen, M., Gauthier, J.C., Audebert, P., Fuchs, J., Meyer-Ter-Vehn, J., Hegelich, M., Karsch, S. & Pukhov, A. (2002). Energetic ions generated by laser pulses: A detailed study on target properties. *Phys. Rev. S.T.A.B.* **5**, 061301.

Sakagami, H., Johzaki, T., Nagatomo, H. & Mima, K. (2006). Fast ignition integrated interconnecting code project for cone-guided targets. *Laser Part. Beams* **24**, 191–198.

Schollmeier, M., Harres, K., Nürnberg, F., Blazevic, A., Audebert, P., Brambrink, E., Fernandez, J.C., Flippo, K.A., Gautier, D.C., Geissel, M., Hegelich, B.M., Schreiber, J. & Roth, M. (2008). Laser beam-profile impression and target thickness impact on laser-accelerated protons. *Phys. Plasmas* **15**, 053101

Schollmeier, M., Roth, M., Blazevic, A., Brambrink, E., Cobble, J.A., Fernandez, J.C., Flippo, K.A., Gautier, D.C., Habs, D., Harres, K., Hegelich, B.M., Hessling, T., Hoffmann, D.H.H., Letzring, S., Nürnberg, F., Schaumann, G., Schreiber, J. & Witte, K. (2007). Laser ion acceleration with micro-grooved targets. *Nucl. Instr. Meth. Phys. Res. A* **577**, 186–190.

SENTOKU, Y., BYCHENKOV, V.Y., FLIPPO, K., MAKSIMCHUK, A., MIMA, K., MOUROU, G., SHENG, Z.M. & UMSTADTER, D. (2002). High-energy ion generation in interaction of short laser pulse with high-density plasma. *Appl. Phys. B* **74**, 207–215.

SEO, J.T., YOO, S.H. & HAHN, S.J. (2007). Effects of underdense preplasma on the energetic proton generation in ultraintense short pulse laser interaction with an overdense plasma slab. *J. Phys. Soc. Jpn* **76**, 114501.

SNAVELY, R.A., KEY, M.H., HATCHETT, S.P., COWAN, T.E., ROTH, M., PHILLIPS, T.W., STOYER, M.A., HENRY, E.A., SANGSTER, C., SINGH, M.S., WILKS, S.C., MACKINNON, A.J., OFFENBERGER, A.A., PENNINGTON, D.M., YASUIKE, K., LANGDON, A.B., LASINSKI, B.F., JOHNSON, J., PERRY, M.D. & CAMPBELL, E.M. (2000). Intense high-energy proton beams from petawatt-laser irradiation of solids. *Phys. Rev. Lett*. **85**, 2945–2948.

STRANGIO, C., CARUSO, A., NEELY, D., ANDREOLI, P.L., ANZALONE, R., CLARKE, R.J., CRISTOFARI, G., DEL PRETE, E., DI GIORGIO, G., MURPHY, C., RICCI, C., STEVENS, R. & TOLLEY, M. (2007). Production of multi-MeV per nucleon ions in the controlled amount of matter mode (CAM) by using causally isolated targets. *Laser Part. Beams* **25**, 85–91.

TABAK, M., HAMMER, J., GLINSKY, M.E., KRUER, W.L., WILKS, S.C., WOODWORTH, J., CAMPBELL, E.M., PERRY, M.D. & MASON, R.J. (1994). Ignition and high gain with ultrapowerful lasers. *Phys. Plasmas* **1**, 1626–1634.

WILKS, S.C., LANGDON, A.B., COWAN, T.E., ROTH, M., SINGH, M.S., HATCHETT, S.P., KEY, M.H., PENNINGTON, D.M., MACKINNON, A.J. & SNAVELY, R.A. (2001). Energetic proton generation in ultra-intense laser-solid interactions. *Phys. Plasmas* **8**, 542–549.

YOGO, A., DAIDO, H., FUKUKI, A., LI, Z., OGURA, K., SAGISAKA, A., PIROZHKOV, S., NAKAMURA, S., IWASHITA, Y., SHIRAI, T., NODA, A., OISHI, Y., NAYUKI, T., FUJI, T., NEMOTO, K., CHOI, Y., SUNG, J.H., KO, D.-K., LEE, J., KANEDA, M. & ITOH, A. (2007). Laser prepulse dependency of proton-energy distributions in ultraintense laser-foil interactions with an online time-of-flight technique. *Phys. Plasmas* **14**, 0431104.